THE DISTRIBUTION OF INORGANIC CATIONS IN MOUSE TESTIS

Electron Microscope and Microprobe Analysis

ABRAHAM L. KIERSZENBAUM, CESAR M. LIBANATI, and CARLOS J. TANDLER

From the Centro de Investigaciones sobre Reproducción, Facultad de Medicina, and the Comisión Nacional de Energía Atómica, and the Instituto de Anatomía General y Embriología, Facultad de Medicina, Buenos Aires, Argentine

ABSTRACT

For localization of pyroantimonate-precipitable cations, mouse testes were fixed with a saturated aqueous solution of potassium pyroantimonate (pH about 9.2, *without* addition of any conventional fixative), hardened with formaldehyde, and postosmicated. A good preservation of the cell membranes and over-all cell morphology is obtained as well as a consistent and reproducible localization of the insoluble antimonate salts of magnesium, calcium, and sodium. Four sites of prominent antimonate deposits are revealed, besides a more or less uniform distribution of the precipitates. These sites are: (*a*) In the walls of the seminiferous tubules, localized in two concentric layers corresponding to the inner and outer layers of the tubular wall; (*b*) Around the blood vessels and adjacent connective tissue; (*c*) At the area of contact between the Sertoli cell and spermatids, where a double line of precipitate surrounds the head of the mature spermatids; and (*d*) In the cell nuclei, disposed between regions of the condensed chromatin. The nucleus of mature spermatids did not show any sign of antimonate precipitation. The implications of this inorganic cation distribution are discussed with relation to their anionic counterparts, their localization in other animal and plant tissues, and the possibility that those sites may represent barriers to the free passage of ions.

INTRODUCTION

Localization of soluble inorganic cations at the subcellular level has been attempted recently by several authors (1–15). In all these cases, the electron microscope has been used for visualizing the electron-opaque deposits formed when a precipitating reagent which contained a heavy atomic element was put in contact with the tissue. The technical difficulties were related to two main problems: (*a*) the possibility of shifts of the ions at the moment of fixation, and (*b*) the precise chemical identification of the precipitate.

The manner in which the first problem was approached—i.e. the precipitation reaction with the tissue—has varied with the different investigators, and the results obtained have not been always in complete agreement (14). These somewhat divergent results are not totally unexpected however, since they reflect precisely the mobilities of the soluble ions. Some procedures used involve a relatively short prefixation with a conventional fixative (7, 13); diffusion or shifts of the ions could occur in this period. Other methods involve the

use of a mixed fixative, i.e. containing both a conventional fixative and the precipitating reagent (e.g., 1. 2, 10); in this case, the effect of the fixative and that of the precipitating reagent on tissue constituents at the moment of fixation cannot be evaluated separately.

Previous work in our laboratory (15–17) has contributed to the concept that some precipitating reagents themselves behave as fixatives (in the sense that the cell morphology is well preserved) and has afforded the opportunity to study the action of the precipitant alone. With these new procedures, heavy precipitates were observed at the subcellular level, and the problem of their chemical identification was approached by selective-area electron diffraction (16) and microprobe analysis (15, 17). It has been demonstrated that in the cell nucleus a concentrated pool of soluble inorganic orthophosphate anions (16, 17) coexists with relatively large amounts of the inorganic cations calcium, magnesium, and sodium (15), and that both types of electrolytes showed a similar pattern of intranuclear localization.

In the present paper, the distribution of inorganic cations in the mouse testis determined by the use of the procedure described previously by Tandler et al. (15) will be reported: a direct fixation in the precipitating reagent, an aqueous saturated solution of potassium pyroantimonate. It was found, in agreement with the results obtained with rat liver and maize rootlets (15), that the cell morphology was strikingly well preserved and that heavy insoluble antimonate precipitates of magnesium, calcium, and sodium were deposited with a definite pattern of localization.

MATERIAL AND METHODS

Adult Swiss mice (Rockland strain) were anesthetized with ether. The testes were quickly dissected free, minced into small pieces in a drop of the fixative at room temperature, and thereafter immersed in a larger amount of the fixative. Another group of mice were previously injected with Mitomycin-C which initiates the repopulation of the seminiferous tubules (A. L. Kierszenbaum. In preparation.), and sacrificed after 14 days.

Electron Microscope Fixation Procedure

The fixative used was a saturated (about 2%, w/v) aqueous solution of potassium pyroantimonate (Riedel-De Haën Ag., Seelze, Hanover, Germany, analytical reagent) freshly prepared by boiling the salt in deionized or twice glass-distilled water, cooling rapidly to room temperature, and centrifuging (pH about 9.2). It was used either immediately or after standing overnight. The tissue was fixed and hardened with formaldehyde as described before (15). In addition, postosmication was also employed in the present study.

The tissue was handled in three ways after the hardening step in the 5% formaldehyde solution in potassium pyroantimonate (15): (*a*) It was washed once with distilled water for 5–10 min at room temperature and twice with ice-cold distilled water for another 10–15 min; or (*b*) It was heated at 90–95°C for 2–5 min in a half-saturated solution of potassium pyroantimonate (15), rapidly cooled, and then washed with ice-cold distilled water for about 15 min; or (*c*) After being washed in distilled water according to procedure (*a*), it was immersed in an ice-cold 2% osmium tetroxide solution in distilled water for 1–2 hr.

In our hands, a 2% osmium tetroxide solution in saturated or half-saturated potassium pyroantimonate was not effective in step (*c*); the tissue did not blacken satisfactorily at the alkaline pH of these solutions. Afterwards, the three types of processed tissues were dehydrated with graded concentrations of cold ethanol, passed through propylene oxide, and embedded in Maraglas (Marblette Corp., Long Island City, N.Y.). Thin sections were cut with glass knives on a Porter-Blum microtome, mounted on Formvar-coated copper grids, and examined *unstained* with a Siemens Elmiskop I electron microscope.

Electron Microprobe

The distribution of the atomic elements in the thick (1 μ) sections was studied with a Cameca model MS 46 X-ray microanalyzer with an accelerating voltage of 20 kv and a probe current of 210 nA. The $L\alpha_1$-radiation was used for antimony, whereas the lighter elements were scanned with the $K\alpha_1$-radiation. The 1 μ Maraglas sections were mounted on formvar-coated copper grids, and these grids were further coated on both sides with a thin film of aluminum (17); the sample can support several hours of impact of the electron beam without damage. The diameter of the probe was about 6 μ, in order to increase the counting rate. The determination of each of the minor constituents took several hours. As has been emphasized before (15), the conditions of analysis are not similar for all the atomic elements and, therefore, the relative proportions of the different cations cannot be judged by comparison of their respective micrographs. On the other hand, the number of specks in a micrograph is proportional to the concentration of the given element at different points in the same micrograph.

RESULTS

Electron Microscope

The most prominent feature to be observed in *unstained*, postosmicated sections of pyroantimonate-fixed tissues is the presence of abundant, electron-opaque precipitates (Figs. 1–7). These precipitates were also evidenced when postosmication was omitted (*insert*, Fig. 1), indicating that the electron opacity is due to antimony; moreover, they were not altered appreciably by heating the tissue at 90–95°C in half-saturated potassium pyroantimonate. This last fact strongly suggests that those precipitates are not formed by deposition of the potassium pyroantimonate itself or by antimonic acid (which forms by lowering the pH of the pyroantimonate solution). These last deposits are easily dissolved by heating in an excess of half-saturated potassium pyroantimonate, whereas the sodium, magnesium, and calcium pyroantimonates are not (as a result of the common-ion effect; 15). Therefore, most of the electron-opaque deposits shown in the electron micrographs must have originated from a precipitation reaction between the pyroantimonate anions of the fixative and the tissue cations. This point is confirmed with the probe analysis (see below).

Over-all tissue and cell structure was strikingly well maintained regardless of the pH of the antimonate reagent and the omission of a conventional fixative in the initial fixation procedure. At present, we have no explanation of how potassium pyroantimonate is able to preserve the tissue and cell integrity; this salt is not a general protein-precipitating reagent, and its alkaline pH probably causes extraction of some biochemical constituents. This is probably the reason why the images given by the postosmicated tissues differ somewhat from those of tissues processed according to the conventional fixation procedure (e.g. the cell nuclei appear less osmicated after pyroantimonate fixation; Figs. 1 and 3). The cell membranes—including the nuclear double membrane (Fig. 3)—are not disrupted (Fig. 1). The maintenance of their integrity helps to explain the ability of the pyroantimonate anion to maintain a large amount of precipitable cations after the cells come into contact with the fixative.

After a prolonged (12–24 hr) immersion in potassium pyroantimonate, the tissue usually did not blacken satisfactorily with osmium tetroxide and the cell membranes remained barely visible, if at all. The factors which influence the loss of osmiophilia were not studied in detail because the primary object of the present work is not affected. In this, the pattern of precipitate deposition has been found to be a constantly reproducible result. All the testes examined, either normal or injected with Mitomycin-C, showed the same four major sites of precipitate deposition, which were:

(*a*) THE CELL NUCLEUS: All the nuclei (Figs. 1 and 3), except those of the mature spermatid (Fig. 6), show the presence of an electron-opaque precipitate located always within the interchromatin regions. A similar pattern of intranuclear localization has been described also in rat liver and in plant material (15). A correlation between the presence of inorganic cations and that of ribonucleoprotein particles has been suggested for the cell nucleus (15). The present finding of the complete absence of cation-antimonate precipitates in sites of high DNA content, i.e. in the nuclei of mature spermatids (Fig. 6), further supports this contention.

(*b*) BLOOD VESSELS: Heavy electron-opaque

In all these figures—except Fig. 8—the testes have been fixed in saturated potassium pyroantimonate alone without addition of any conventional fixative, hardened with formaldehyde, postosmicated, and embedded in Maraglas. Staining was always *omitted*.

FIGURE 1 Survey electron micrograph of a thin section of mouse testis illustrating the massive cation-antimonate precipitates at the boundary of the seminiferous tubule, around the blood vessels (*bv*), in the connective tissue, and in the nuclei. In the tubular wall, the precipitate is localized in the two noncellular layers; *Fb*, a nucleus in the intermediate layer of the tubular wall. *Ley*, Leydig cell. Scale mark, 5 μ. × 4,000.

Insert: Thin section of part of a seminiferous tubule in which postosmication was *omitted*, showing the antimonate precipitates in two nuclei (*N*) and in a portion of the tubular wall (arrow). Scale mark, 1 μ. × 6,000.

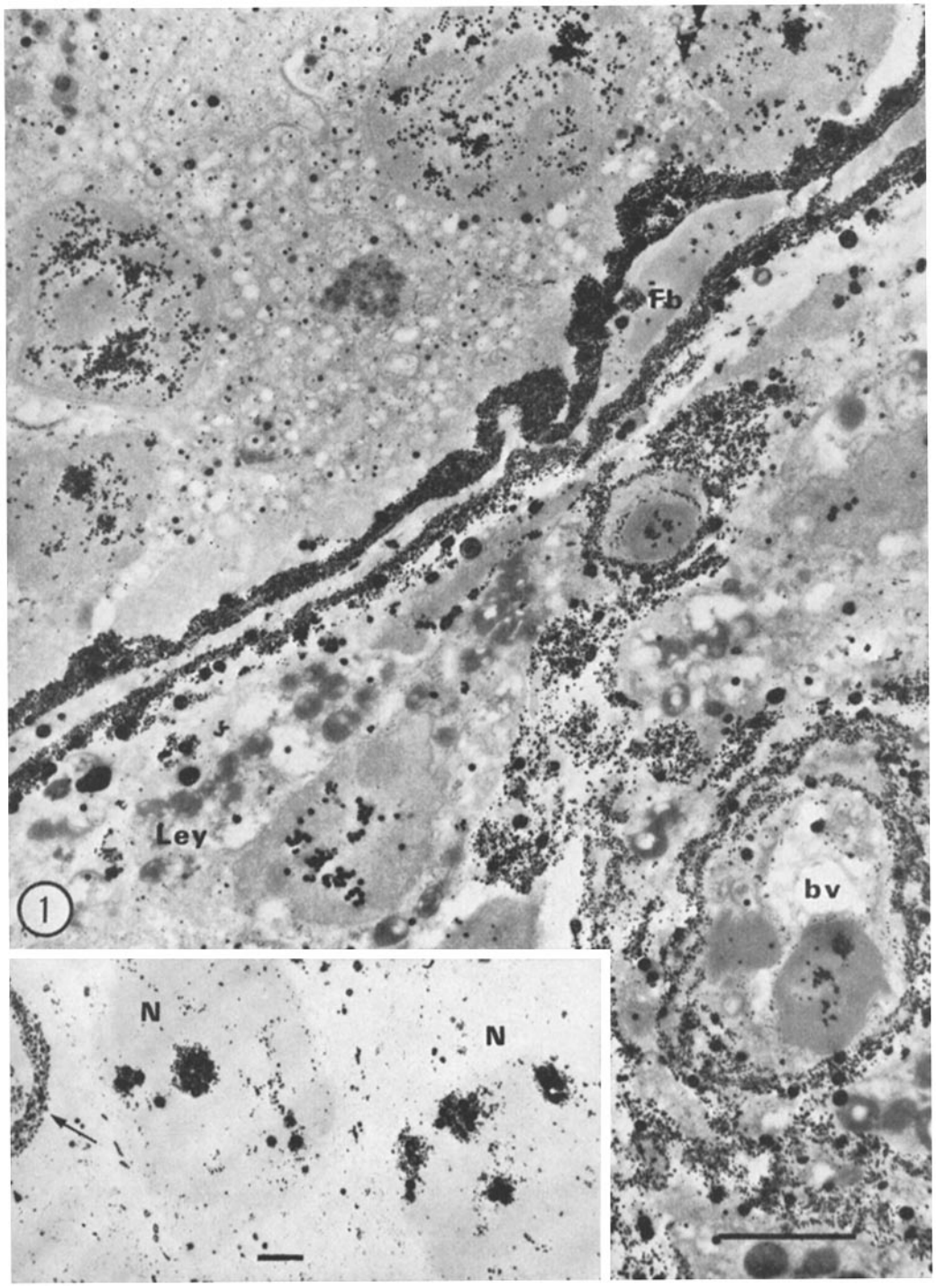
Fb
Ley
bv
1
N
N

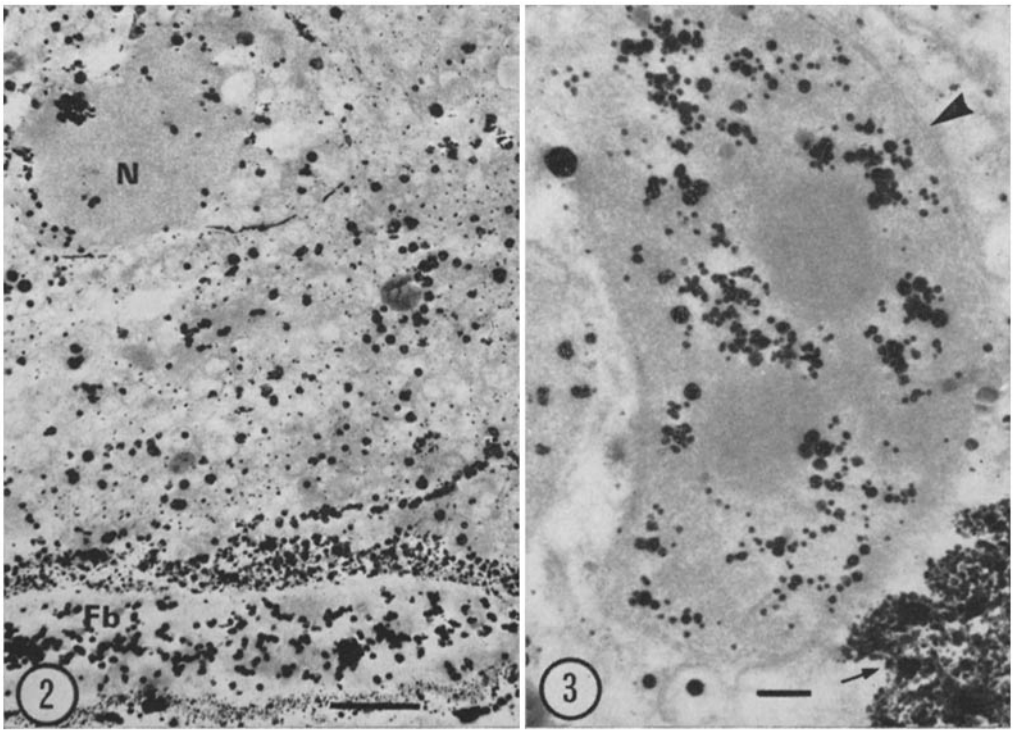

FIGURE 2 Same as Fig. 1, showing cation-antimonate precipitates in the inner layer of the tubular wall, in the cytoplasm of the germinal epithelium, and in the nucleus of a fibroblast (*Fb*) lying in the central layer of the tubular wall. The nucleus of an immature spermatid (*N*) is also seen. Scale mark, 2 μ. × 6,000.

FIGURE 3 Same as Fig. 1, higher magnification, showing the precipitate in the nucleus of the Sertoli cell and in the inner layer of the tubular wall (arrow). The two round masses of condensed chromatin are free of precipitate. The nuclear membrane (arrowhead) is continuous and two layers can be discerned. Scale mark, 0.5 μ. × 14,000.

precipitates are found around all the blood vessels in the intertubular space (Figs. 1 and 4). In many cases, a double line of precipitate surrounding the endothelial and perivascular cells is evident (Fig. 4). Usually, the antimonate precipitate also extends over regions of the connective tissue which accompanies the blood vessels (Fig. 1).

The antimonate precipitate is also encountered in the nuclei of the endothelial and perivascular cells, in accordance with what is observed in all nuclei, as described above. A similar pattern of antimonate precipitation has been also observed in the blood vessels of the rat liver (15). Many of the small blood vessels have collapsed during the procedure of mincing the testis into small pieces and have lost their content; this is the reason why the lumen is barely visible in Figs. 1 and 4 and is also free of antimonate precipitate.

(*c*) THE WALL OF THE SEMINIFEROUS TUBULES: Heavy antimonate deposits are found at the boundary of the seminiferous tubules, i.e. in the tubular walls. The precipitates are disposed in two concentric layers (Fig. 1) which enclose a space relatively free of precipitate; the fibroblasts which constitute this last layer show appreciable amounts of precipitate mainly in their nuclei (Fig. 2). This "sandwiched" pattern of antimonate deposition occurs all along the seminiferous tubules and corresponds to the two mucoprotein-containing layers described in the tubular walls by Clermont (18). In the internal layer, some striations are noted in the disposition of the antimonate deposits; at higher magnifications, they are seen to follow the pattern of the collagen (or reticulin; 19) fibrils sectioned tangentially.

(*d*) RELATIONSHIPS BETWEEN SERTOLI

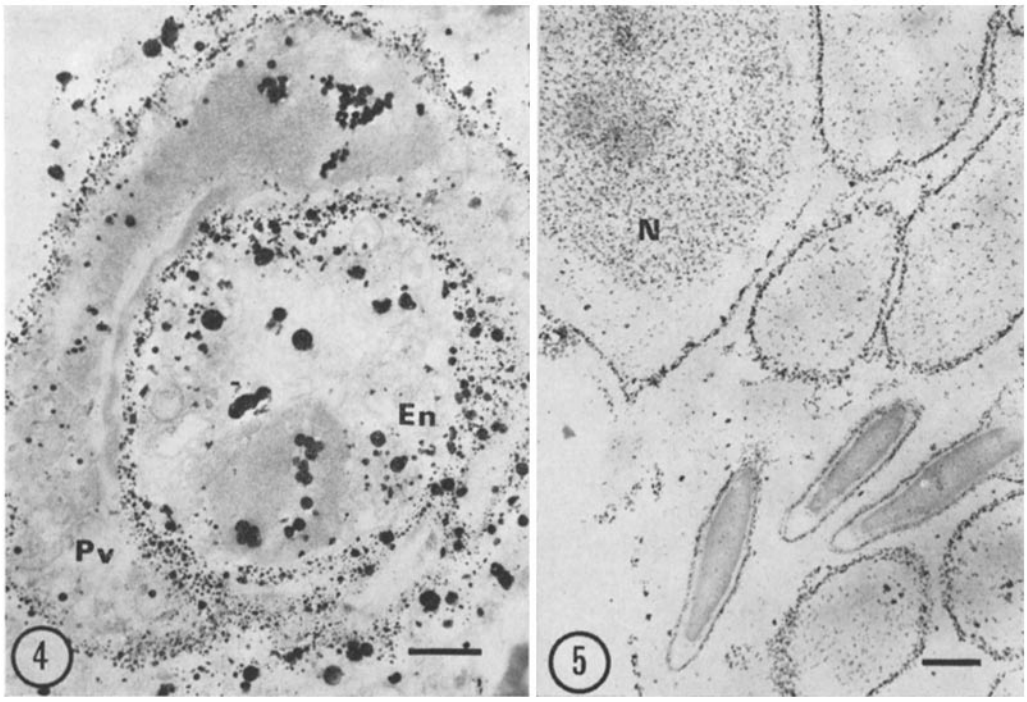

FIGURE 4 Electron micrograph of a small blood vessel. A double layer of precipitate is discernible around the endothelial (*En*) and the perivascular (*Pv*) cells, as well as within their respective nuclei. Scale mark, 1 μ. × 10,000.

FIGURE 5 Electron micrograph of testis fixed in 10% formaldehyde and immersed afterwards in potassium pyroantimonate, showing redistribution of the precipitate; this is localized more uniformly along all the plasma membranes and within the nucleus (*N*), and is almost absent in the nuclei of mature spermatids. Postosmication omitted. Scale mark, 1 μ. × 7,500.

CELL AND SPERMATIDS: The area in which the heads of the maturing spermatids lie in contact with the apical cytoplasm of the sustentacular Sertoli cells was filled with a heavy precipitate (Fig. 6). At higher magnifications, this precipitate appears usually as a double line of precipitate (Fig. 7). Its precise localization is difficult to ascertain, but it is not present in the acrosome.

The morphology of this region is shown in Fig. 8 as it appears after a conventional glutaraldehyde–osmium tetroxide fixation. At the head of the spermatid, the closely apposed plasma membranes of the spermatid and the Sertoli cell are in close contact, leaving between them a very small intercellular space. In the Sertoli cell, a thin layer of cytoplasm disposed along the spermatid head shows electron-opaque fibrillar material disposed along it. This fibrillar material has been described previously by several authors (20–22). The double layer of antimonate precipitate must be located somewhere between the plasma membrane of the spermatid and the vacuolized areas of the Sertoli cell (Fig. 8), i.e. including the thin cytoplasmic layer of the Sertoli cell surrounding the spermatid. The antimonate precipitate also appears around the immature spermatids, although it is less conspicuous. Electron-opaque deposits can be discerned also between the groups of mature spermatids and disposed around their tails (Fig. 6).

In addition to the precipitate in these four major sites of deposition, a more uniformly dispersed precipitate can be visualized in the cytoplasm of the Sertoli and germinal cells (Figs. 1 and 2). It is composed of granules of different sizes, and some of the larger ones are apparently formed by aggregation of smaller granules. It reflects a lower concentration of cations in the cytoplasm and

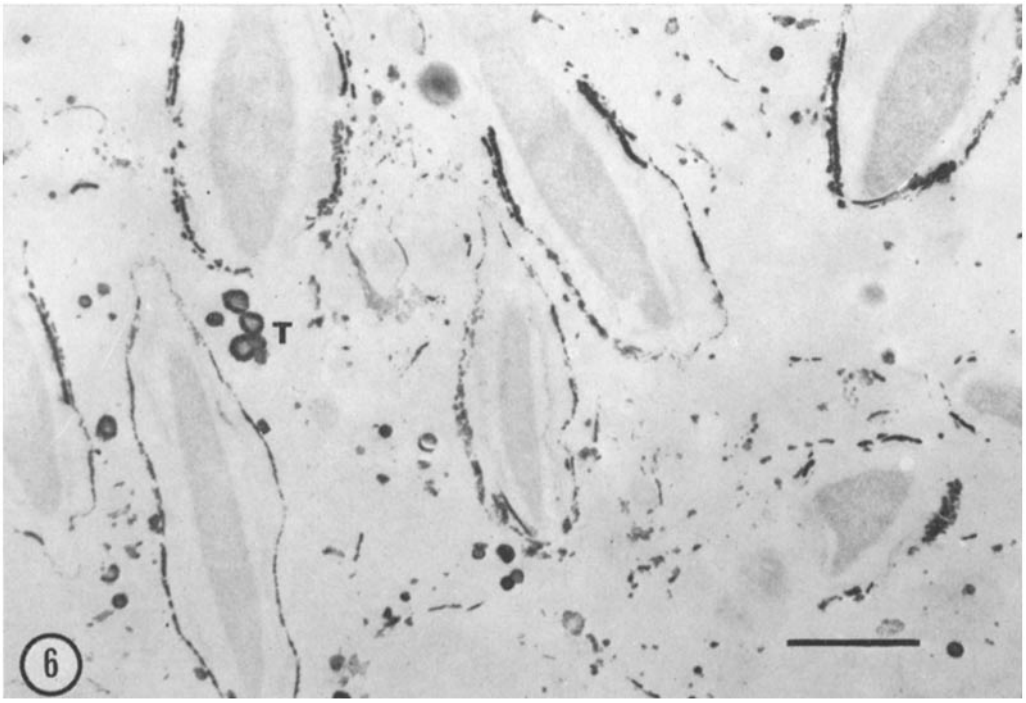

FIGURE 6 Same as Fig. 1, showing the area in which the mature spermatids lie in contact with the Sertoli cell. A heavy precipitate encircles all the heads of the spermatids and their tails (*T*). The nuclei of the spermatids do not show any sign of antimonate deposition. Scale mark, 1 μ. × 12,500.

probably also traces of the fixative which resisted the washing procedure.

Fig. 5 illustrates the result obtained when diffusion artifacts are induced, e.g. by fixing the testis overnight in an unbuffered ice-cold solution of 10% formaldehyde, washing briefly in cold distilled water, and thereafter immersing in saturated potassium pyroantimonate. Electron-opaque antimonate deposits were observed along all the plasma membranes and within the nuclei (except the nuclei of mature spermatids which are relatively free of precipitate). It is evident that this pattern of antimonate deposition is quite different from that described previously and represents a more "homogeneous" pattern of distribution; those sites in which heavy deposits have been localized by a direct fixation in pyroantimonate (e.g. the seminiferous tubules and around the mature spermatids) are not so conspicuous here, showing that some redistribution has occurred. This last pattern of localization (Fig. 5) is considered artifactual, because it was obtained under conditions which certainly permit a shift of the diffusible ions. Besides this, a staining effect of the pyroantimonate anion was observed to take place (e.g. the nuclei of mature spermatids [Fig. 5] and red blood cells).

Electron Microprobe

Fig. 9 shows the antimony L α_1-emission image of a thick (1 μ) section of mouse testis fixed in potassium pyroantimonate and embedded in Maraglas. The outlines of the boundaries of two seminiferous tubules are evident and show the presence of antimony in the tubular walls as several discrete masses in the seminiferous tubules and intertubular space. This topography can be visualized in more detail in Fig. 1 which shows a similar image in the electron microscope.

Figs. 10–12 show, respectively, the Kα_1-emission images of the lighter elements sodium, calcium, and magnesium in the same area. Their distribution correlates with that of the antimony, indicating the presence of these cations in the antimonate precipitates.

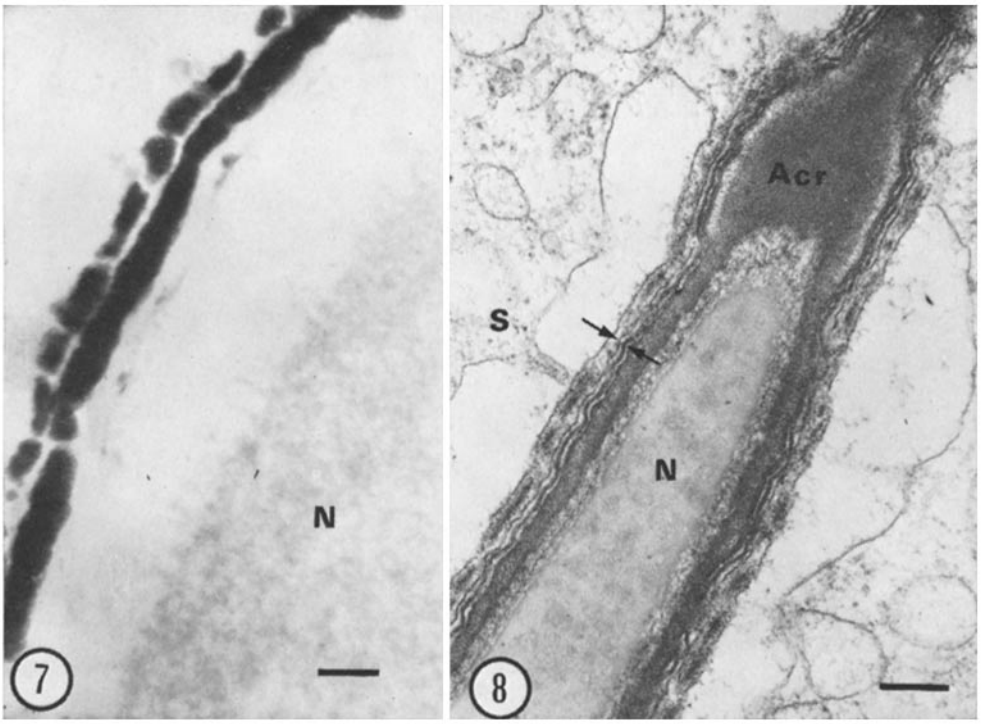

FIGURE 7 Same as Fig. 6, higher magnification, illustrating the double line of precipitate around the mature spermatid. The acrosome is unstained. *N*, nucleus. Scale mark, 0.1 μ. × 80,000.

FIGURE 8 Thin section of a mature spermatid fixed in glutaraldehyde, postosmicated, and stained with uranyl acetate and lead citrate. It illustrates the thin layer of Sertoli cytoplasm contacting the spermatid and containing electron-opaque fibrillar material along it. The plasma membranes of the Sertoli cell (*S*, arrow) and that of the spermatid (arrow) leave a small intercellular space. *N*, nucleus. *Acr*, acrosome. Scale mark, 0.2 μ. × 44,000.

DISCUSSION

The present paper, together with the evidence presented in a previous paper (15), demonstrates that immersion of living cells into an aqueous-solution of potassium pyroantimonate (*alone*, without addition of any conventional fixative) resulted in a massive precipitation of the insoluble salts of magnesium, calcium, and sodium and a strikingly good preservation of the tissue and cell morphology. This is a constantly reproducible result in all the specimens tested and in several animal and plant tissues (15). How these effects are achieved by the pyroantimonate anion is completely unknown at present. Tisher et al. (14) reported recently the extremely good preservation of the tissue and overall cell structure after a short in vivo exposure to potassium pyroantimonate and suggested the possibility that the pyroantimonate anion is capable of entering the cell prior to fixation. We have now established that the pyroantimonate anion is not only capable of entering the cell but that it behaves itself as a fixative. A saturated or a half-saturated solution and a solution whose pH was lowered to about 8.2 behave almost similarly (15). The saturated solution has the advantage of having the maximum amount of the pyroantimonate anion in solution.

The question remains whether the localizations obtained reflect the in vivo sites. The fact that the pattern of localization is different from that obtained artifactually (Fig. 5), i.e. where shifts of the ions are prone to occur by prefixation and washing in water, strongly supports—although does not prove—the validity of the localizations obtained. In

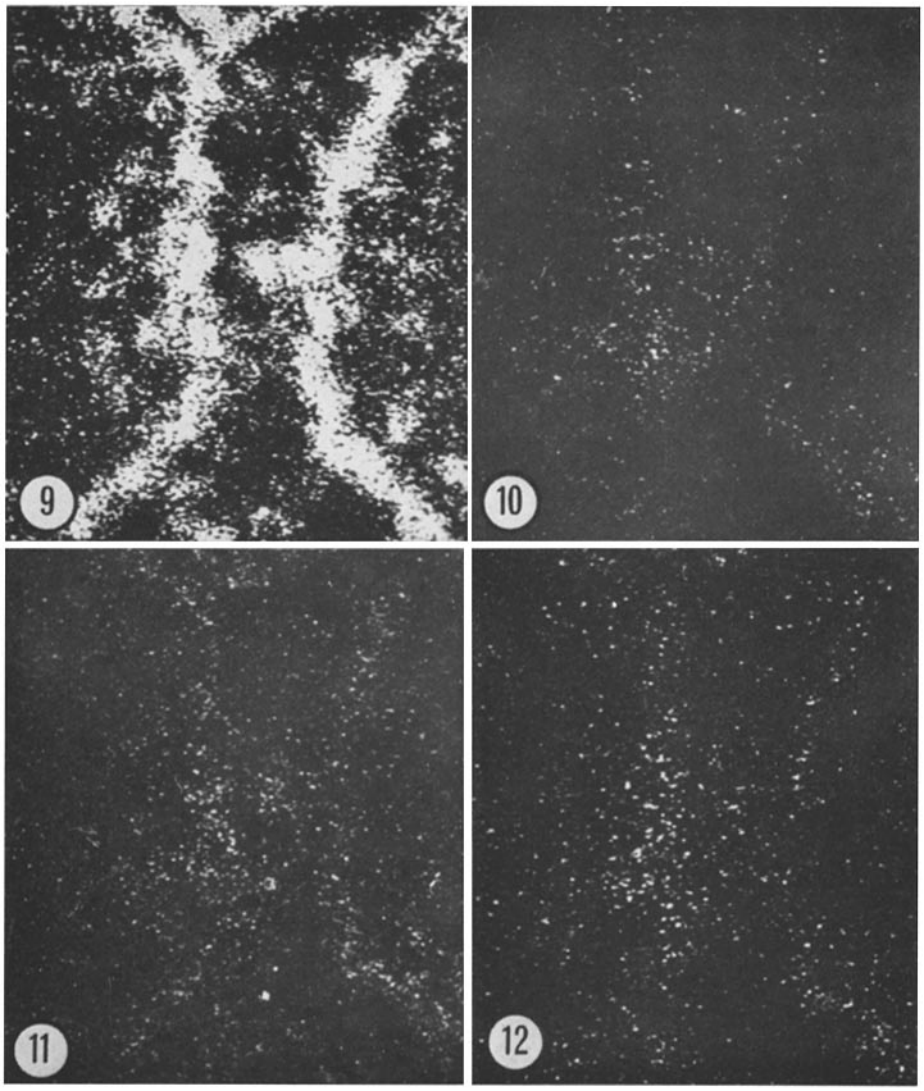

FIGURE 9 The image for the $L\alpha_1$-emission wavelength of antimony from a thick 1 μ section of mouse testis fixed in potassium pyroantimonate. The outlines of two tubular walls are evident. × 750.

FIGURES 10–12 The images for the $K\alpha_1$-emission wavelength of sodium, calcium, and magnesium, respectively, on the same area of the section shown in Fig. 9. × 750.

the testis, other approaches seem feasible, particularly at the tissue level; e.g. the concentration of inorganic cations in the wall of the seminiferous tubules should be revealed by freezing-drying and subsequent probe analysis, but this has not been attempted here.

As a working hypothesis, we have suggested that, at those sites in which a heavy precipitate has been localized, some macromolecule(s) having ion-binding capacities or an ion-exchange character is involved (15, 16). The chemical alterations introduced by the conventional fixatives alter this property and produce shifts of the "bound" ions. On the other hand, some salts probably do not affect this binding capacity so drastically, at least during the time of fixation. In this manner, and within certain limits, the precipitating pyroantimonate anions could reach these sites more quickly

than the cations could escape from them. One can speculate that some conditions of cellular integrity should be fulfilled also; the preservation of the integrity of cell membranes after immersion in potassium pyroantimonate (Figs. 1 and 3) probably also plays a role.

In the cell nucleus, and particularly in the nucleolus of maize rootlets, a large pool of inorganic phosphate anions has been demonstrated (16, 17) to coexist with the inorganic cations (15). In spite of the high concentration of the orthophosphate ions (17) and probably of the divalent cations, too (15), calcium phosphate precipitates apparently are not formed in vivo under normal conditions.

Besides the nucleus, other loci in which heavy cation-antimonate precipitates have been localized (around the blood vessels, mature spermatids, and the wall of seminiferous tubules; Figs. 1 and 6), represent sites in which a barrier to the free diffusion of soluble ions is expected to occur. It is probable that these loci are a reflection of some constituents having a high affinity or binding capacity for inorganic cations; in this manner, these loci bind inorganic cations strongly and could act, owing to the cations' positive charge, as a barrier to cation transport. A number of studies have indicated the existence of barriers to the passage of several substances between the plasma and the seminiferous tubules (23, 24) and have suggested that it is located at the tubular wall (25). The acid mucoprotein(s) known to be present in the two concentric layers of the tubular walls (18) is a possible candidate for the postulated macromolecule having a high binding capacity for inorganic cations; the localization of the antimonate-reactive cations Mg^{++}, Ca^{++}, and Na^{+} seems to correspond closely to that of the periodic acid–Schiff positive mucoprotein.

This investigation was supported by a grant from the Consejo Nacional de Investigaciones Científicas y Técnicas, Argentine and The Population Council, Inc., New York. Dr. Tandler is an established Investigator of the CNICT, Argentine.

The authors wish to express their thanks to Mr. Hector Espejo for assistance in the operation of the microanalyzer.

Received for publication 18 May 1970, and in revised form 20 July 1970.

REFERENCES

1. KOMNICK, H. 1962. *Protoplasma.* **55**:414.
2. KOMNICK, H., and U. KOMNICK. 1963. *Z. Zellforsch. Mikrosk. Anat.* **60**:163.
3. KAYE, G. I., J. D. COLE, and A. DONN. 1965. *Science (Washington).* **150**:1167.
4. KAYE, G. I., H. O. WHEELER, R. T. WHITLOCK, and N. LANE. 1966. *J. Cell Biol.* **30**:237.
5. NOLTE, A. 1966. *Z. Zellforsch. Mikrosk. Anat.* **72**:562.
6. ZADUNAISKY, J. A. 1966. *J. Cell Biol.* **31**:C11.
7. HARTMANN, J. F. 1966. *Arch. Neurol.* **14**:633.
8. SPICER, S. S., J. H. HARDIN, and W. B. GREENE. 1968. *J. Cell Biol.* **39**:216.
9. BULGER, R. E. 1969. *J. Cell Biol.* **40**:79.
10. LEGATO, M. J., and G. A. LANDER. 1969. *J. Cell Biol.* **41**:401.
11. LANE, B. P., and E. MARTIN. 1969. *J. Histochem. Cytochem.* **17**:102.
12. HARDING, J. H., S. S. SPICER, and W. B. GREENE. 1969. *Lab. Invest.* **21**:214.
13. SIEGESMUND, K. A. 1969. *J. Anat.* **105**:403.
14. TISHER, C. C., W. J. CIRKSENA, A. U. ARSTILA, and B. F. TRUMP. 1969. *Amer. J. Pathol.* **57**:231.
15. TANDLER, C. J., C. M. LIBANATI, and C. A. SANCHIS. 1970. *J. Cell Biol.* **45**:355.
16. TANDLER, C. J., and A. J. SOLARI. 1969. *J. Cell Biol.* **41**:91.
17. LIBANATI, C. M., AND C. J. TANDLER. 1969. *J. Cell Biol.* **42**:754.
18. CLERMONT, Y. 1958. *Exp. Cell Res.* **15**:438.
19. LACY, D., and J. ROTBLAT. 1960. *Exp. Cell Res.* **21**:49.
20. BRÖKELMANN, J. 1961. *Anat. Rec.* **139**:211.
21. HORSTMANN, E. 1961. *Z. Zellforsch. Mikrosk. Anat.* **54**:68.
22. FLICKINGER, C. J. 1967. *Z. Zellforsch. Mikrosk. Anat.* **78**:92.
23. REISIN, I. L. 1969. Passage and distribution of substances through the seminiferous tubules in rat testis. Doctoral Thesis, Faculty of Medicine, University of Buenos Aires.
24. MANCINI, R. E., A. CASTRO, and A. C. SEIGUER. 1967. *J. Histochem. Cytochem.* **15**:516.
25. SETCHELL, B. P. 1967. *J. Physiol. (London).* **189**:63P.